

## FT-ICR STUDY OF CHEMICAL REACTION OF SILICON CLUSTER WITH NITRIC OXIDE

Shigeo Maruyama\*, Shuhei Inoue\*\* and Masamichi Kohno\*

\*Engineering Research Institute, The University of Tokyo  
2-11-16 Yayoi, Bunkyo-ku, Tokyo 113-8656, Japan

\*\*Department of Mechanical Engineering, The University of Tokyo  
7-3-1 Hongo, Bunkyo-ku, Tokyo 113-8656, Japan

**ABSTRACT** Chemical reaction of small silicon cluster ions ( $\text{Si}_n^+$ :  $20 \leq n \leq 29$ ) with nitric oxide was studied by using the FT-ICR (Fourier Transform Ion Cyclotron Resonance) mass spectrometer. Silicon clusters were generated by a pulsed laser-vaporization supersonic-expansion cluster beam source directly connected to the FT-ICR mass spectrometer. Injected and size selected clusters were thermalized to the room temperature through collisions with argon, and were exposed to the reactant gas in the ICR cell. As a result, extraction reaction of a silicon atom was observed. When SiO was removed from  $\text{Si}_n^+$  cluster, resulting  $\text{Si}_{n-1}N^+$  clusters occasionally fragmented into smaller pieces. For a comparison, laser induced fragmentation patterns of size-selected clusters were performed. The reaction induced fragmentation was explained that after the Si atom extraction, resulting  $\text{Si}_{n-1}N^+$  fragmented in the same manner as pure  $\text{Si}_{n-1}^+$  clusters when the released heat of the initial reaction was not absorbed in the  $\text{Si}_{n-1}N^+$  clusters.

**Keywords:** Silicon Cluster, Chemical Reaction, FT-ICR, Mass Spectroscopy, Nitric Oxide

### 1. NOMENCLATURE

<i>B</i> :	Magnetic field
<i>f</i> :	Ion cyclotron resonance frequency
<i>M</i> :	Cluster ion mass
<i>m</i> :	Number of silicon atoms of a cluster
<i>n</i> :	Number of silicon atoms of a cluster
<i>q</i> :	Charge of cluster ion

### 2. INTRODUCTION

Recently atomic and molecular clusters are recognized as playing an important role in the thin-film deposition process and various phase-change phenomena. Furthermore, small size clusters are the most adequate system for the verification of quantum molecular dynamics calculations such as the interference of light and matter. Here, the understandings of silicon surface reaction are crucial for the thin-film technology such as the CVD deposition process using silane ( $\text{SiH}_4$ ) as the starting material. Silicon clusters formed in the gas phase before deposition in CVD process are suggested to have essential effect on the quality of the thin film product. Furthermore, since most of chemical reagent is not attacking the perfect (111)-(7×7) surface during the deposition process, the adequate modeling of chemical reaction for atomically irregular surface is demanded. Silicon clusters are best material to compare the theoretical modeling with experimental results.

On the other hand, silicon clusters have been extensively studied in order to understand how the

properties of a bulk material change as atomic dimensions are approached. It is well known that such efforts for carbon clusters lead to the discovery of fullerene and nanotube [1]. Geometrical and electronic structures of very small silicon clusters with less than 8 atoms have been well understood by recent progress in theoretical [2,3] and experimental studies [4,5]. Difficulty in *ab initio* calculations increased exponentially for larger clusters with increase in complexity of electronic structure and geometrical configurations that need to be considered.

Hence, most of *ab initio* or density functional calculations have been tried for the geometric configurations based on physical insight [2]. Simulated annealing technique [3] or genetic algorithm [6] with Car-Parrinello molecular dynamics with LDA approximation, tight-binding molecular dynamics or classical molecular dynamics have been tried, as well. Experimentally, the practical preparation of size-selected clusters larger than 8 atoms has been possible with the laser-vaporization cluster beam source. Smalley and co-workers have probed chemical reaction with ammonia [7,8], ethylene [9,10], and trimethylamine [11] with the Fourier transform ion cyclotron resonance (FT-ICR) mass spectrometer. On the other hand, Jarrold [12] and co-workers have extensively studied chemical reaction with ethylene [13,14],  $\text{O}_2$  [15], water [16], and ammonia [17,18] using the ion drift tube apparatus. They also measured the mobility of clusters and distinguished some geometric isomers [19-23]. There has been a serious controversy between results of these 2 groups. From FT-ICR reaction experiments with ammonia and ethylene,  $\text{Si}_{33}$ ,  $\text{Si}_{39}$ , and  $\text{Si}_{45}$

were demonstrated to be unreactive. However, ion drift tube experiments showed completely no specialty in these cluster sizes. In spite of many efforts to explain this controversy such as laser annealing [10, 11] and collision induced annealing experiments [12], it is still unclear.

Based on the design concept of Smalley's group [9-11, 24], we have implemented a new FT-ICR spectrometer with direct injection cluster beam source [25-28]. And we have studied the chemical reaction of  $\text{Si}_n^+$  ( $11 \leq n \leq 20$ ) with ethylene [28], because most of experiments with FT-ICR concentrated on silicon clusters larger than 30. Even though we didn't implement the laser annealing, the preliminary results were in good agreement with Jarrold's in this small cluster size range.

In this paper, the chemical reaction with nitric oxide is reported. The reaction process was completely different from those with ethylene

### 3. EXPERIMENTAL APPARATUS

The experimental apparatus implemented are similar to Smalley's group [9-11, 24] and the detailed characteristics are described in elsewhere [25-28]. Fig. 1

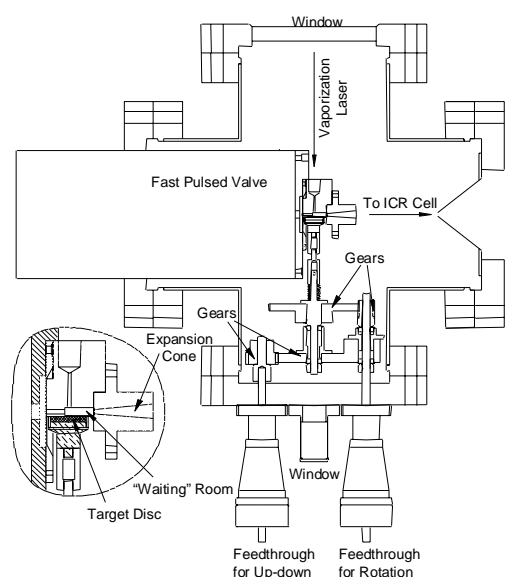


Fig. 1 Laser-vaporization cluster beam source.

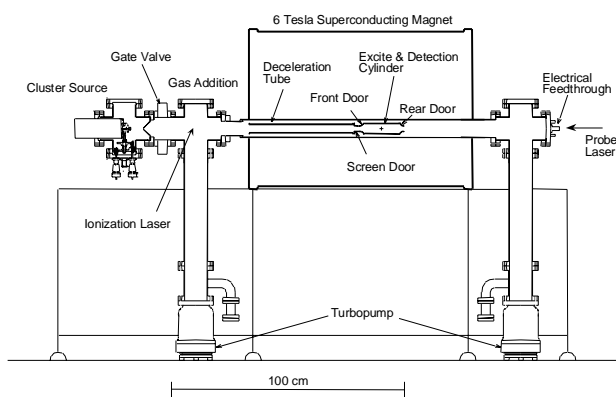


Fig. 2 FT-ICR apparatus with direct injection cluster beam source.

and Fig. 2 show the cluster beam source and direct injection FT-ICR apparatus, respectively. The silicon cluster ion beam was generated outside of magnetic field by the laser-vaporization cluster beam source shown in Fig. 1. A pulsed gas valve, the sample motion mechanism and a skimmer were installed in a 6-inch 6-way UHV cross. A solid sample disk was vaporized by the focused beam of Nd: YAG laser (2nd Harmonics) while timed pulsed gas was injected to the nozzle. In the atmosphere of helium gas, vaporized atoms condensed to clusters, and then, were carried and cooled by the supersonic expansion of helium gas. The cluster beam was directly injected to the magnetic field through a skimmer with the opening diameter of 2 mm and a deceleration tube [24].

The FT-ICR is the unique mass spectroscopy based on the ion-cyclotron motion of clusters in a strong magnetic field. The ion cyclotron frequency  $f$  is inversely proportional to the ion mass  $M$  as follows.

$$f = \frac{qB}{2\pi M} \quad (1)$$

Extremely high mass-resolution at high mass-range such as resolution of 1 amu at 10,000 amu range can be obtained. Furthermore, since the ions can be trapped in the vacuum for a few minutes, it is possible to perform the chemical reaction experiments. The ICR cell, 42 mm I.D. 150 mm long cylinder was placed in a stainless tube (SUS316) of 84 mm I.D. which penetrated the homogeneous 5.87 Tesla super conducting magnet commercially available for NMR. Two turbo-pumps (300  $\ell/s$ ) fore-pumped by a smaller turbo-pump of 50  $\ell/s$  were placed at the floor in order to avoid the effect of strong magnetic field. The typical background pressure was  $3 \times 10^{-10}$  Torr.

The typical experimental procedure of reaction was as follows:

- Cluster beam was injected in 10 Hz for 10 s to the ICR cell. Size range of cluster ions was roughly selected by the deceleration voltage [24] as discussed in section 4.1.
- The kinetic energy of clusters was thermalized to room temperature with argon gas. This procedure was skipped for present study.
- Unwanted clusters were over-excited and excluded from ICR cell by SWIFT (Stored Waveform Inverse Fourier Transform) excitation [8, 29].
- Remaining clusters were thermalized with room temperature argon gas at  $10^{-5}$  Torr for 5 s.
- Nitric oxide gas with typically  $10^{-6}$  Torr was injected to the cell by 10 Hz pulsed valve for predetermined reaction time period.
- After pumping out for about 8 to 10 s, cluster ions were excited to detect the mass distribution.

## 4. RESULTS AND DISCUSSION

### 4.1 Generated silicon clusters

Fig. 3 shows typical silicon cluster ion mass spectra depending on the deceleration voltage. By applying the pulsed deceleration voltage when cluster ions are in the deceleration tube, the cluster ions lose corresponding

translational energy. Since the kinetic energy of cluster ions at the supersonic velocity of helium is almost proportional to their mass, the cluster ions that can enter the ICR cell with fixed door voltage are roughly selected by this deceleration technique. No special size distribution such as well known in carbon clusters [1] was observed. There were only a little bit contamination signals in between pure silicon clusters. More detailed view is shown in Fig. 4. A spectrum measured with “dirty” cluster source condition is compared with the calculated isotope distribution based on

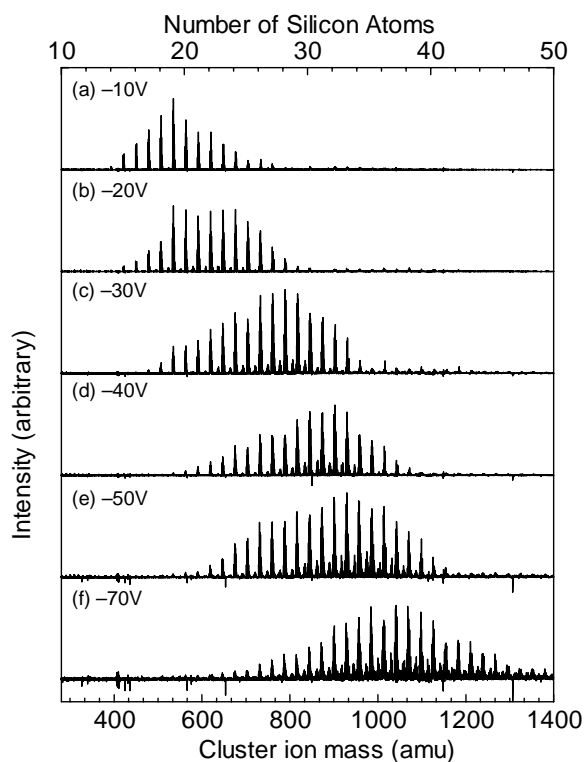


Fig. 3 As injected silicon cluster mass spectra depending on the deceleration voltage.

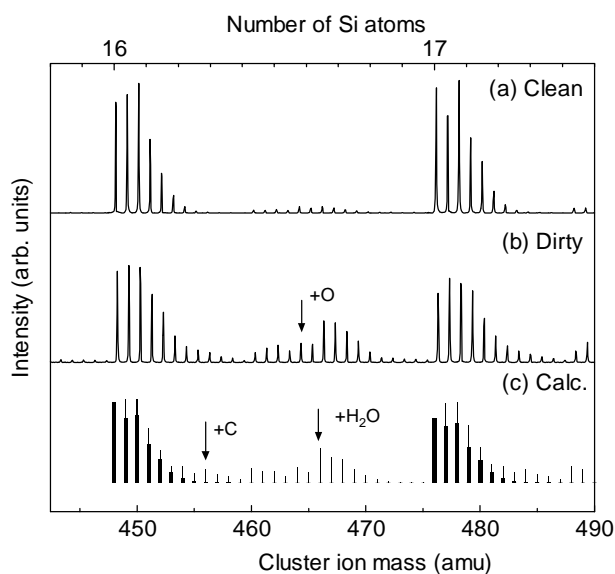


Fig. 4 Contamination with  $\text{H}_2\text{O}$ , C, O, and H. A slightly thicker line in (c) represent pure silicon isotopes.

the natural abundance of silicon isotopes. Apparent contaminants for “clean” condition (expanded view of Fig. 3) were hydrogen, carbon and oxygen atoms. It seems that water molecules sticking in helium carrier gas line and sample surface caused all contamination except for carbon. The small amount of carbon contamination was due to the carbon cluster experiments performed previously. It seems that water molecules were dissociatively chemisorbed on silicon clusters. Here, the worst contaminants must be H and  $\text{H}_2$ , because they could not be distinguished in most of ion mass detectors in practical experimental conditions. Even with FT-ICR experiments, careful and painful examinations were necessary.

#### 4.2. Chemical reaction with nitric oxide

Fig. 5(a) shows the FT-ICR mass spectrum of the injected and trapped silicon clusters. In order to observe the chemisorption reaction product on a clean baseline, all clusters except for desired size ( $\text{Si}_{20}^+$ ) were excited away from the ICR cell by the selective RF excitation called “SWIFT” technique [8,29]. Clusters were well thermalized to the room temperature by exposures to argon at a pressure at  $1 \times 10^{-5}$  Torr for 5 seconds (about 1000 collisions) after SWIFT. Fig. 5(b) shows the mass spectrum measured after this mass selection. Fig. 5(c) shows the spectrum after the exposure of  $\text{Si}_{20}^+$  to nitric oxide at  $1 \times 10^{-6}$  Torr for 1 second. To our surprise, destructive chemisorption of nitrogen atom was observed. It seems that most of  $\text{Si}_{20}^+$  were destructed by nitric oxide with a tiny amount of  $\text{Si}_{20}^+$  left. Fig. 5(d) shows the results after 5 seconds exposure. Since the reaction rate was much faster than our experience with ethylene, we could not observe the time dependence of reaction for this experiment. At this stage, we could not understand what reaction process from  $\text{Si}_{20}^+ + \text{NO}$  led to  $\text{Si}_{12}\text{N}^+$ .

Fig. 6 shows the reaction results for  $\text{Si}_{24}^+$  with nitric oxide. Exactly the same procedure of reaction was done as for  $\text{Si}_{20}^+$  in figure 5. In this case, the reaction process could be simply understood. As nitric oxide attached to the cluster, a silicon atom was extracted probably as  $\text{SiO}$ . This reaction

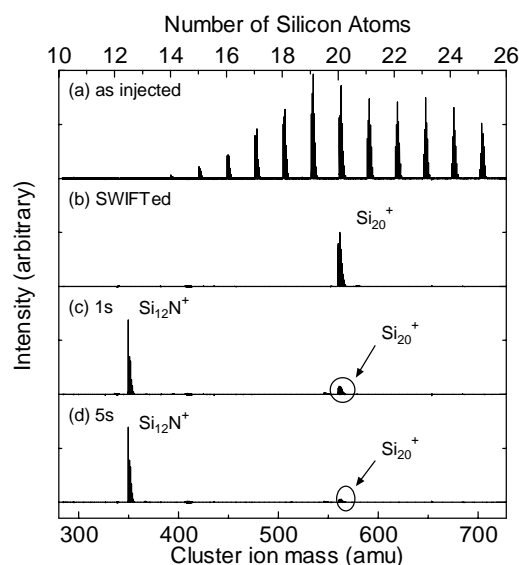
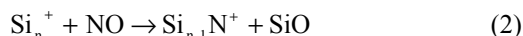


Fig. 5 FT-ICR spectra of reaction of  $\text{Si}_{20}^+$  with nitric oxide.

can be expressed as follows.



This reaction was also very fast and we could not resolve time dependence of reaction with this pressure of NO. Compared to the typical chemisorption rate of ethylene, the reaction rate was more than 100 times faster. Probably the reaction was so fast that NO reacted to the cluster at every collision.

Results of reaction for all size tested ( $20 \leq n \leq 29$ ) are summarized in Fig. 7. It is clear that small size clusters (except for  $\text{Si}_{21}^+$ ) were broken into smaller pieces, but large size clusters followed the reaction (2). It seems that initial reaction for  $\text{Si}_{20}^+$ ,  $\text{Si}_{22}^+$ , and  $\text{Si}_{23}^+$  is also in reaction (2), because the products always have a nitrogen atom. A simple interpretation of results is follows. Afterwards the larger size cluster could absorb the energy of exothermic

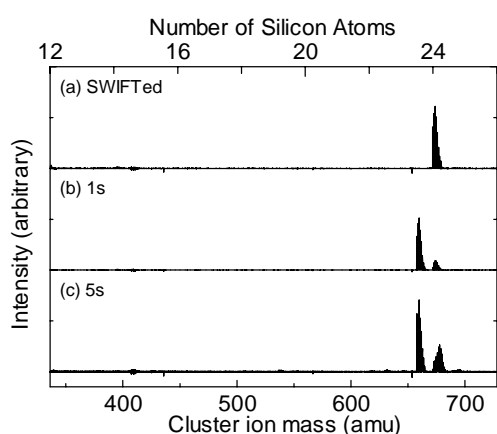


Fig. 6 FT-ICR spectra of reaction of  $\text{Si}_{24}^+$  with nitric oxide.

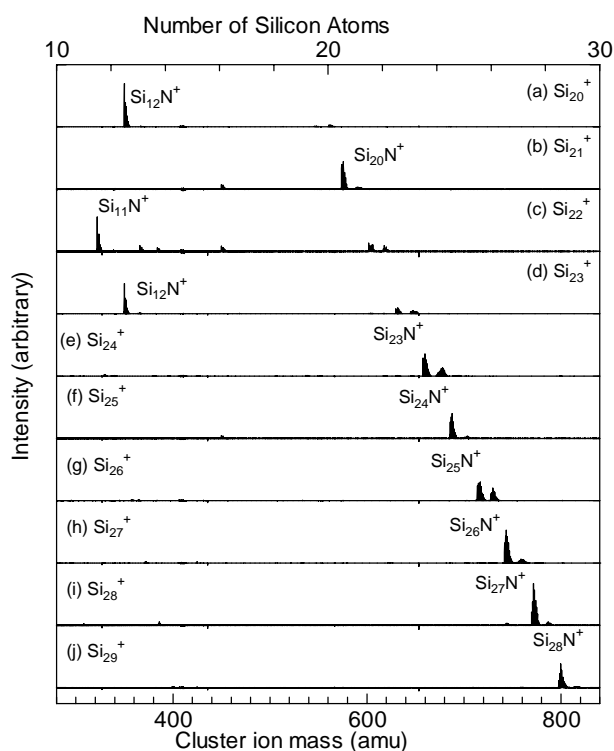


Fig. 7 Chemical reaction of silicon cluster with nitric oxide.

reaction in its vibrational modes. But the smaller cluster came to the dissociation without sufficiently absorbing the thermal energy. However it is also possible that original geometric structure difference selected these two paths. Jarrold *et al.* [30] reported geometric structure of silicon cluster changed around 25 size in their ion drift experiment. They suggested the elongated sausage-like structure for clusters smaller than this threshold size and the more spherical structure for larger clusters.

### 4.3. Laser photo-fragmentation of silicon cluster

Since the fragmentation process seemed to be involved in some of reactions, laser photo-fragmentation experiments were performed. As well as reaction experiments size-selected clusters were trapped in the ICR cell by SWIFT technique. They were thermalized to the room temperature by collisions with argon and irradiated with 3rd harmonic of Nd: YAG laser at  $2\text{mJ}/\text{cm}^2$  for 2 seconds. The laser light was mildly focused with 1m focused lens from right hand side in Fig. 2. Photo-fragment product ions are shown in Fig. 8 with some "parent" ions left in the cell. These results were almost perfectly consistent with previously reported fragmentation results by laser photo-fragmentation [30], and collisional fragmentation with rare gas molecules [31]. Table 1 shows the summary of present and previous works. Laser photo-fragmentation experiments by Zhang *et al.* [31], labeled "Laser" in table 1, were performed with the tandem time-of-flight apparatus with the similar cluster source as present. Size selected cluster ions were irradiated with the 4th harmonics of YAG laser during their field free flight. They reported that the wavelength of probe laser was not important by trying wavelength such as 2nd (532nm), 3rd (355nm) harmonics of Nd: YAG, KrF (249nm) and ArF (193nm). The bold face type shows the major daughter ions. The collision induced fragmentation, labeled "Collision",

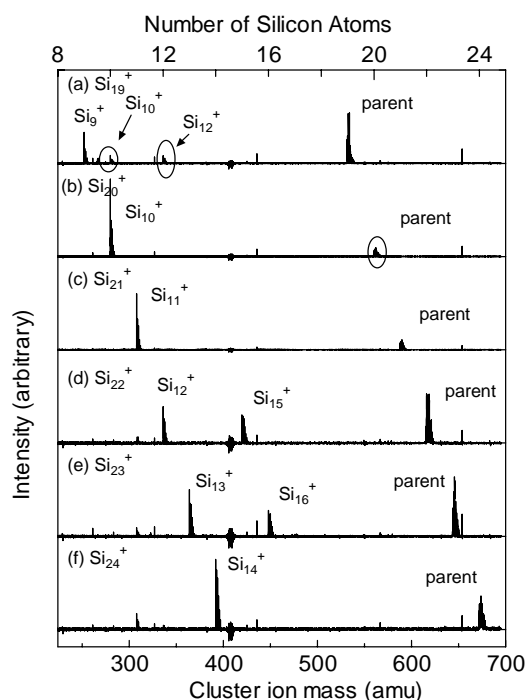
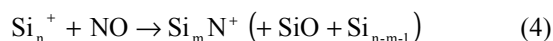


Fig. 8 Photo-fragmentation results for size-selected clusters.

summarized by Shvartsburg et al. [32] were measured with the ion drift apparatus. Size selected cluster ions were accelerated into the argon buffer gas section. Because the ionization potential of a cluster is generally higher for larger cluster, it is assumed that larger fragment keeps the positive charge as follows.



It should be noticed that the fragmentation patterns are perfectly consistent with different experiments. Then, it can be assumed that these fragmentation patterns are simply due to the thermodynamic process. The "React" in present results compiles the number of silicon atoms  $m$  of clusters observed in our reaction induced fragmentation as follows.



At first look at table 1, the reaction induced fragmentation seems completely different from all other "normal" fragmentation results. However, the reaction-induced fragmentation pattern can be regarded as the same as "normal" with the following assumption. We assume that the initial extraction reaction (2) takes place for all clusters. Then, the resultant ion  $\text{Si}_{n-1}\text{N}^+$  may have sufficient thermal energy due to the exothermic initial reaction for self-fragmentation. Then, we further assume that the fragmentation of  $\text{Si}_{n-1}\text{N}^+$  is similar to  $\text{Si}_{n-1}^+$ , i.e., the chemisorbed N atom doesn't affect the fragmentation. With these assumptions, the reaction-induced fragmentation patterns are comparable to the photo-fragmentation patterns. For example, original  $\text{Si}_{22}^+$  reacted as reaction (2) to give  $\text{Si}_{21}\text{N}^+$ , then, fragmented to  $\text{Si}_{11}\text{N}^+$  just as  $\text{Si}_{21}^+$  fragmented to  $\text{Si}_{11}^+$ . Some differences of the reaction-induced fragmentations from photo-fragmentations are observed for  $\text{Si}_{22}\text{N}^+$ .  $\text{Si}_{22}\text{N}^+$  selected only one dominant daughter,  $\text{Si}_{12}\text{N}^+$ , in contrast to that  $\text{Si}_{22}^+$  photo-fragmented to  $\text{Si}_{12}^+$  and  $\text{Si}_{15}^+$  in almost the same rate. It should be explained that the reaction induced fragmentation was the result of the fixed amount of the reaction energy that was near the threshold of the fragmentation. Hence, the fragmentation process with lower activation energy was selected. This result is consistent with the primary product  $\text{Si}_{12}^+$  by the collision-induced fragmentation [32], which is argued to give lower energy fragmentation channel compared with laser photo-fragmentation. The same explanation can be applied to the case of  $\text{Si}_{20}^+$ . Since it is not easy to control the excitation energy for photo-fragmentation and collision induced fragmentation experiments, this reaction-induced fragmentation can be regarded as the ideal threshold fragmentation experiment. The very sharp difference in the fragmentation patterns for 20 to 23 size range in our results

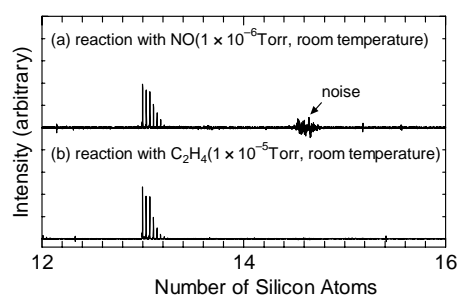


Fig. 9 Reactivity of  $\text{Si}_{13}^+$ .

in Fig. 7 should be excellent information of changes in binding energy of silicon clusters. We expect the lower energy fragmentation channel for  $\text{Si}_{19}$ ,  $\text{Si}_{21}$ , and  $\text{Si}_{22}$  compared with  $\text{Si}_{20}$ ,  $\text{Si}_{23}$  and larger clusters.

#### 4.4. Specialty of $\text{Si}_{13}^+$

Since the specialty of  $\text{Si}_{13}^+$  was well known as unreactive clusters, we had performed the NO reaction experiment for  $\text{Si}_{13}^+$  in comparison to our previous ethylene reaction [28]. The result is shown in Fig. 9. With the reaction condition that all other clusters considerably reacted, only  $\text{Si}_{13}^+$  was completely unreactive to ethylene nor NO. These results further confirmed the specialty of  $\text{Si}_{13}^+$ . It may be a special unreactive cluster, that could be isolated as the bulk material.

## 5. CONCLUSION

Chemical reaction of size-selected small silicon clusters ( $\text{Si}_n^+$ :  $20 \leq n \leq 29$ ) in the FT-ICR apparatus was performed. With the collision of NO to the cluster ion  $\text{Si}_n^+$ , SiO was removed and  $\text{Si}_{n-1}\text{N}^+$  was left in the ICR cell. Depending on the cluster size, resulting  $\text{Si}_{n-1}\text{N}^+$  further fragmented into smaller cluster due to the initial exothermic reaction energy. This fragmentation pattern was compared with the laser photo-fragmentation experiments in the ICR cell. It was suggested that this reaction-induced fragmentation experiments could be regarded as the threshold fragmentation experiments and gave much information about the original structure and binding energy of small silicon clusters.

## 6. ACKNOWLEDGEMENT

Part of this work was supported by Grant-in-Aid for Scientific Research (B) (No. 12450082) and for Encouragement of Young Scientists (No. 11750155) from the Ministry of Education, Science, Sports and Culture, Japan.

## 7. REFERENCES

Table 1 Fragmentation of Si cluster

n	present		Laser [31]	Collision [32]
	React	Laser		
15		8, 9	8, 9	<b>8, 9</b>
16		10	<b>10</b> , 6, 4	<b>10</b> , 6
17		10, 11	<b>10</b> , 11, 7	<b>10</b> , 11
18		11	<b>11</b> , 15, 17, 8	<b>11</b>
19		9, 10, 12	<b>9</b> , 10, 6, 7, 12, 13, 16	<b>9</b> , 12
20	12	10	<b>10</b> , 6-11	<b>10</b>
21	(20)	11	<b>11</b> , 6-10	<b>11</b>
22	11,(21)	12, 15	12, 15, 10, 6	<b>12</b> , 15
23	12	13, 16	10, 13, 11, 16, 6, 7	<b>13</b> , 16
24	(23)	14	<b>14</b> , 11, 7, 10	<b>14</b> , 7, 11

- [1] H. W. Kroto, J. R. Heath, S. C. O'Brien, R. F. Curl and R. E. Smalley,  $C_{60}$ : Buckminsterfullerene, *Nature*, 318-14 (1985), pp. 162-163.
- [2] K. Raghavachari and C. M. Rohlfing, Bonding and Stabilities of Small Silicon Clusters: A Theoretical Study of  $Si_7$ - $Si_{10}$ , *J. Chem. Phys.*, 89-4 (1988), pp. 2219-2234.
- [3] M. Ramakrishna and A. Bahel, Combined Tight-Binding and Density Functional Molecular Dynamics Investigation of  $Si_{12}$  Cluster Structure, *J. Chem. Phys.*, 104 (1996), pp. 9833-9840.
- [4] E. C. Honea, A. Ogura, D. R. Peale, C. Felix, C. A. Murray, K. Raghavachari, W. O. Sprenger, M. F. Jarrold, and W. L. Brown, Structures and Coalescence Behavior of Size-Selected Silicon NanoClusters Studied by Surface-Plasmon-Polariton Enhanced Raman Spectroscopy, *J. Chem. Phys.*, 110-24 (1999), pp. 12161-12172.
- [5] S. Li, R. J. Van Zee, W. Weltner, Jr, and K. Raghavachari,  $Si_3$  –  $Si_7$ . Experimental and theoretical Infrared Spectra, *Chem. Phys. Lett.*, 243 (1995), pp. 275-280.
- [6] K-M. Ho, A. A. Shvartsburg, B. Pan, Z-Y. Lu, C-Z. Wang, J. G. Wacker, J. L. Fye, and M. F. Jarrold, Structure of Medium-Sized Silicon Clusters, *Nature*, 392-9 (1998), pp. 582-585.
- [7] J. L. Elkind, J. M. Alford, F. D. Weiss, R. T. Laaksonen, and R. E. Smalley, FT-ICR Probes of Silicon Cluster Chemistry: The Special Behaviors of  $Si_{39}^+$ , *J. Chem. Phys.*, 87-4 (1987), pp. 2397-2399.
- [8] J. M. Alford, R. T. Laaksonen, and R. E. Smalley, Ammonia Chemisorption Studies on Silicon Cluster Ions, *J. Chem. Phys.*, 94-4 (1991), pp. 2618-2630.
- [9] L. R. Anderson, S. Maruyama and R. E. Smalley, Ethylene Chemisorption on Levitated Silicon Cluster Ions: Evidence for the Importance of Annealing, *Chem. Phys. Lett.*, 176-3,4 (1991), pp. 348-354.
- [10] S. Maruyama, L. R. Anderson and R. E. Smalley, Laser Annealing of Silicon Clusters, *J. Chem. Phys.*, 93-7 (1990), pp. 5349-5351.
- [11] S. Maruyama, L. R. Anderson and R. E. Smalley, Laser Annealing of Semiconductor Clusters: Trimethylamine Reactions with Positive and Negative Clusters, *Mat. Res. Soc. Symp. Proc.*, 206 (1991), pp. 63-70.
- [12] M. F. Jarrold, Silicon Cluster Ions, *Cluster Ions*, Ed. C. Y. Ng, T. Bear and I. Powis, John Wiley & Sons (1993), pp. 165-215.
- [13] M. F. Jarrold, J. E. Bower, and K. Creegan, Chemistry of Semiconductor clusters: A Study of the Reactions of Size Selected  $Si_n^+$  ( $n = 3-24$ ) with  $C_2H_4$  Using Selected Ion Drift Tube Techniques, *J. Chem. Phys.*, 90-1 (1989), pp. 3615-3628.
- [14] K. M. Creegan and M. F. Jarrold, Chemistry of Semiconductor Clusters: Reactions of  $Si_n^+$  ( $n = 11-50$ ) with  $C_2H_4$  Show Evidence for Numerous Structural Isomers, *J. Am. Chem. Soc.*, 112 (1990), pp. 3768-3773.
- [15] M. F. Jarrold, U. Ray, and K. M. Creegan, Chemistry of Semiconductor Clusters: Large Silicon Clusters Are Much Less Reactive Towards Oxygen than the Bulk, *J. Chem. Phys.*, 93-1 (1990), pp. 224-229.
- [16] U. Ray and M. F. Jarrold, Reactions of Silicon Cluster Ions,  $Si_n^+$  ( $n = 10-65$ ), with Water, *J. Chem. Phys.*, 94-4 (1991), pp. 2631-2639.
- [17] U. Ray and M. F. Jarrold, Interaction of Silicon Cluster Ions with Ammonia: The kinetics, *J. Chem. Phys.*, 93-8 (1990), pp. 5709-5718.
- [18] M. F. Jarrold, Y. Ijira, and U. Ray, Interaction of Silicon Cluster Ions with Ammonia: Annealing, Equilibria, High Temperature Kinetics, and Saturation Studies, *J. Chem. Phys.*, 94-5 (1991), pp. 3607-3618.
- [19] M. F. Jarrold and V. A. Constant, Silicon Cluster Ions: Evidence for a Structural Transition, *Phys. Rev. Lett.*, 67-21 (1991), pp. 2994-2997.
- [20] M. F. Jarrold and J. E. Bower, Mobilities of Silicon Cluster Ions: The Reactivity of Silicon Sausages and Spheres, *J. Chem. Phys.*, 96-12 (1992), pp. 9180-9190.
- [21] M. F. Jarrold and E. C. Honea, Dissociation of Large Silicon Clusters: The Approach to Bulk Behavior, *J. Phys. Chem.*, 95 (1991), pp. 9181-9185.
- [22] K-M. Ho, A. A. Shvartsburg, B. Pan, Z-Y. Lu, C-Z. Wang, J. G. Wacker, J. L. Fye, and M. F. Jarrold, Structure of Medium-Sized Silicon Clusters, *Nature*, 392-9 (1998), pp. 582-585
- [23] R. R. Hudgins, M. Imai, M. F. Jarrold, and P. Dugourd, High-Resolution Ion Mobility Measurements for Silicon Cluster Anions and Cations, *J. Chem. Phys.*, 111-17 (1999), pp. 7865-7870.
- [24] S. Maruyama, L. R. Anderson and R. E. Smalley, Direct Injection Supersonic Cluster Beam Source for FT-ICR Studies of Clusters, *Rev. Sci. Instrum.*, 61-12 (1990), pp. 3686-3693.
- [25] S. Maruyama, T. Yoshida, and M. Kohno, FT-ICR Studies of Laser Desorbed Carbon Clusters, *Trans. JSME*, B65-639 (1999), pp. 3791-3798.
- [26] S. Maruyama, T. Yoshida, M. Kohno and M. Inoue, FT-ICR Studies of Laser Desorbed Carbon Clusters, 5th ASME/JSME Thermal Eng. Conf., San Diego, AJTE99-6513 (1999).
- [27] S. Maruyama, H. Kinbara, H. Hayashi, and D. Kimura, Photo-Ionized TOF Mass Spectrometry of Atomic Clusters, *Micro. Thermophys. Eng.*, 1-1 (1997), pp. 39-46.
- [28] S. Maruyama, M. Kohno, S. Inoue, FT-ICR Study of Chemical Reaction of Silicon Clusters, *Therm. Sci. Eng.*, 7-6 (1999), pp. 69-74.
- [29] A. G. Marshall and F. R. Verdun, *Fourier Transforms in NMR, Optical, and Mass Spectrometry*, Elsevier, Amsterdam (1990).
- [30] R. R. Hudgins, M. Imai, M. F. Jarrold, P. Dugourd, High-resolution Ion Mobility Measurements for Silicon Cluster Anions and Cations, *J. Chem. Phys.*, 11-17, (1999), pp. 7865-7870.
- [31] Q. L. Zhang, Y. Liu, R. F. Curl, F. K. Tittel, and R. E. Smalley, Photodissociation of Semiconductor Positive Cluster Ions, *J. Chem. Phys.*, 88, 1988, pp. 1670-1677.
- [32] A. A. Shvartsburg, M. F. Jarrold, B. Liu, Z.-Y. Lu, C.-Z. Wang, and K.-M. Ho, Dissociation Energies of Silicon Clusters: A Depth Gauge for the Global Minimum on the Potential Energy Surface, *Phys. Rev. Lett.*, 81-21, (1998) pp. 4616-4619.